Accepted for publication in Journal of Materials Science

Published in January 3, 2013

DOI: 10.1007/s10853-012-7097-4

Investigation of fiber/matrix adhesion: Test speed and specimen shape effects in the cylinder test

B. Morlin[a], L. M. Vas[a], T. Czigany[a,b,*]

[a]Department of Polymer Engineering, Faculty of Mechanical Engineering, Budapest University of Technology and Economics, Muegyetem rkp. 3., H-1111 Budapest, Hungary

[b]MTA–BME Research Group for Composite Science and Technology, Muegyetem rkp. 3., H-1111 Budapest, Hungary

*corresponding author: czigany@eik.bme.hu

Abstract: The cylinder test, developed from the microdroplet test, was adapted to assess the interfacial adhesion strength between fiber and matrix. The sensitivity of cylinder test to pull-out speed and specimen geometry was measured. It was established that the effect of test speed can be described as a superposition of two opposite, simultaneous effects which have been modeled mathematically by fitting two parameter Weibull curves on the measured datas. Effects of the cylinder size and its geometrical relation on the measured strength values have been analyzed by finite element method. It was concluded that the geometry has a direct influence on the stress formation. Based on the results achieved, recommendations were given on how to perform the novel single fiber cylinder test.

Keywords: adhesive joints, interfacial strength, micromechanical methods, size effect, Speed effect, modelling

Introduction

Fiber reinforced polymers have become substantial structural materials due to the considered effects of elastic matrix and high strength reinforcement. An indispensable prerequisite of this is the presence of an acceptable fiber/matrix adhesion otherwise the load transfer between the two components will not be satisfactory and the expected mechanical properties cannot be realized. Therefore the knowledge of the fiber/matrix adhesion is essential for the calculation of mechanical properties of composites during the design phase [1-5]. The interfacial shear strength as a characteristic of adhesion can be determined by different micromechanical (or single fiber) tests among which the microdebond method is usually preferred [6-11]. The cylinder test, developed by us (see Fig. 1), can be considered as a variant of the microdroplet test [12], that eliminates basic disadvantages of the original method and diminishes some related disturbing effects related to test configuration. Thus, errors due to uncertainties of droplet shape and size, major stress variations arising around the supporting points of the fixing blades and concomitant deformations [13, 15, 19] could be eliminated with specific cylinder geometry. With the cylinder configuration the sensitivity of the method, influenced significantly by the skill of the personnel, could be markedly reduced. Note that the blades are not touching anymore directly the droplet (Fig. 1/a) but a metal plate with a borehole (containing the specimen) which guarantees a “smooth” loading (Fig. 1/b). All these modifications improved significantly the reliability and repeatability of the test.

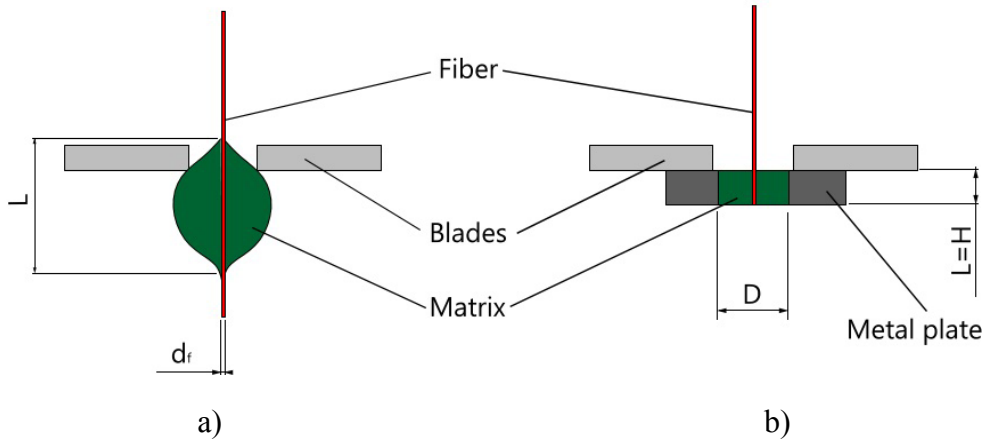

Fig. 1. Microdroplet (a) and cylinder (b) tests, where L: embedded fiber length, H: plate thickness, D: borehole diameter, d_f : fiber diameter

The interfacial shear strength is, of course, influenced by the test parameters, such as the pulling or test speed, specimen size and shape (geometrical proportions). In spite of this, only few authors investigated the effects of these testing conditions. Some results are presented in Table 1. Based on the literature data [13-15] it can be concluded that only few authors investigated the effects of specimen size/test configuration and pulling speed. The main reason for this is probably linked with the first contact between the blade and droplet, which may result in off-axis loading, especially at higher deformation rates. It is also due to uncertainties in respect to the droplet shape that few studies were devoted to measure the effect of blade distance. It is noteworthy that with changing diameter of the droplets different stresses arise even at identical blade distances.

In an earlier article [12] we had reported that the interfacial shear strength depends strongly on the test conditions. Therefore the major goal of this paper this was to get a deeper understanding for probable reasons of the strength variations caused by the effects of variations in the cylinder geometry (embedded fiber length (L), and the cylinder diameter (D), see Fig. 1.), and in the test speed using real tests, finite element modeling and related mathematical description.

Ref	Materials	Measuring Circumstances					Goal of researchers
Zinck et al. [13]	GF EP	Deformation rate [mm/min]	0.05	0.5	5	-	find the optimal mathematical model to evaluate
		τ [MPa]	46.0	80.0	52.0	-	
Straub et al. [14]	Kevlar49 EP	Deformation rate [mm/min]	0.1	2	10	100	determination of the temperature sensitivity, presented results on 21°C
		τ [MPa]	18.5	20.0	15.8	9.0	
Day and Rodrigez [15]	Kevlar49 EP	Blade distance [μm]	20	50	80	-	study of the effect of distance fixing blades and sample size
		τ [MPa]	15.7	15.8	15.5	-	

Table 1. Some literature results of changing different measuring circumstances [13-15]

Materials and methods

For our fiber/matrix interfacial shear strength tests glass fiber (Saint-Gobain RT310 0001 100) and unsaturated polyester (UP) resin of Viapal VUP 4627 BEMT type containing 2 wt% cobalt-naphthanate accelerator and 1.5 wt% Butanox M50 (methyl-ethyl-ketone-peroxide) catalyst were used. EBRECYL 860 additive was used to plasticize the resin. Note that this is an epoxidized and acrylated soyabean oil which may be used to "dilute" unsaturated polyester resins [16]. Cylinder tests were performed with reduced interfacial adhesion, as well. In the latter case the surface of the fibers was treated by Szilorol M-100 type silicone oil ("oiled fibers"). The test specimens were post-cured at 85°C for 2 hours. The embedding plates were made of aluminum, their thickness was H=120-300 μm, the diameter of the borehole was D=240-500 μm.

Geometrical dimensions of the cylinder test configurations were determined by an Olympus BX51 (Hamburg, Germany) optical testing microscope. The matrix was sheared off by Zwick

Z005 (Ulm, Germany) type universal tester using a special droplet removing device [17, 18] at room temperature. Electron micrographs were made on EOL JSM-6380LA (Tokyo, Japan) type electron microscope, with gold coated specimens. The interfacial shear strength (IFSS) value was determined according to as the ratio of deboning force and embedded surface of fiber [15, 17]:

Results and discussion

Effect of test speed

The interfacial shear strength as a function of test speed is depicted in Fig. 2 for the cylinder tests performed. The traces in Fig. 2 suggest that the results are the sum of two processes: one of them monotonically decreasing, whereas the other monotonically increasing the IFSS between GF and UP with increasing test speed (deformation rate).

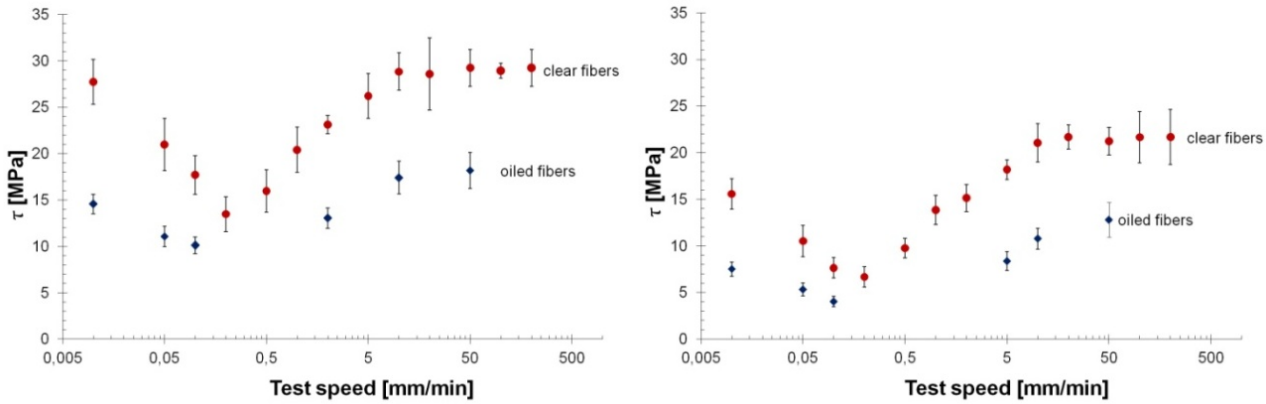

a) b)

Fig. 2. Interfacial shear strength vs. test speed for glass fiber/UP (a) and for glass fiber/ modified UP (with EBECRYL 860) (b) matrix materials, in both cases silicone oil modified interface points are included

In order to decide whether the observations hold only for a given material pair or eventually of general character, the test series done in our earlier article [12] (see Fig. 2/a) was repeated for the UP resin plasticized with 10% EBECRYL 860 (Fig. 2/b). This plasticizing significantly deteriorated the interfacial properties: the strength values became lower whereby

keeping the shape of the original curve (cf. Figs. 2/a and 2/b). Based on the theoretical considerations (which will be introduced later) the tests were done also on "oiled fibers" (i.e. interfacial interactions reduced by using silicone oil) at selected speeds (see Fig. 2).

Theoretical considerations

The monotonically decreasing contribution, deduced from Fig. 2, is related to the matrix-fiber interaction, more exactly to the interfacial bonds. According to certain ideas [19] the molecular chains at the interface (realizing adhesion bonds) – which can be considered tie molecules – are mostly coiled. In case of slow loading there is enough time for relaxation, therefore the tie molecules may stretch as springs and detach, but if the loading is slow enough, they may reattach at other places (see Fig. 3). This can be modeled by the deformation and failure behavior of a yarn consisting of fibers of strong waviness [20].

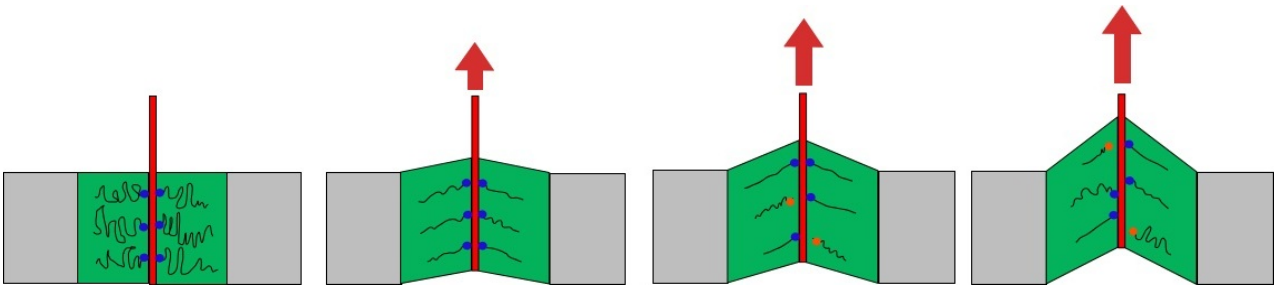

Fig. 3. Explanation of active tie molecules at low speed: (a) starting position, (b) molecular chains extended by stress, (c) detachment and relaxation of individual chains, (d) recombination of the adhesive bonds of relaxed chains in new position

If the test speed is increased then the number of recombined adhesive bonds decreases and finally diminishes. At higher deformation rates the number of extended molecular chains capable of bearing stress also decreases. To sum up, the number of active tie molecules decreases with increasing rate and they become more "rigid", so the deformation gradually shifts closer to the matrix layer adjacent to the fiber surface. The volume of the active zone

increases and thus more molecular chains are deformed. This is associated with an increase in strength and explains the positive (increasing) component until the saturation speed (~10 mm/min, the speed at which the asymptotic shear strength is approximated well) of the traces of results on Fig. 2.

To prove this hypothesis the fiber surface was coated by silicone oil to prevent the formation of active tie molecules at the fiber/matrix interphase. In this case the interfacial shear strength decreased, as expected, while retaining its curve shape as a function of the test speed (see Fig. 2). At lower deformation rates, however, less stress enhancement was experienced than for "non-oiled" fibers. The possible reason for that is that the number of the active tie chains decreased but forces caused by other effects (such as surface roughness, curing shrinkage etc.) remain unaltered. This reduced the sensitivity of the system response to the decreasing deformation rate.

According to our expectations the SEM micrographs made of the test specimens after the fiber removal at low deformation rates (0.01 mm/min) did not show any residual deformation (Fig. 4/a), while at high crosshead speed (200 mm/min) a conical residual deformation (indicated by white circle) can be observed at the entrance of the fiber indicating the presence of an extended deformation zone (Fig. 4/b).

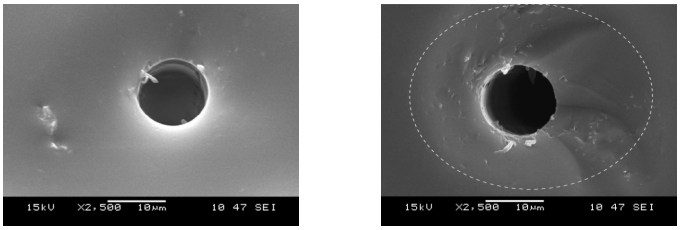

a) b)

Fig. 4. The space left by the removed fiber at deformation rates of (a) 0.01 mm/min and (b) 200 mm/min for glass fiber/UP matrix pair

Mathematical description of the test speed effect

According to the above discussion based on the results in Fig. 2. the shear strength measured in the microbond test is the sum of two contributions (Equation (1)):

$$\tau(v) = \tau_1(v) + \tau_2(v) \qquad (1)$$

where $\tau_1(v)$ is the initial, $\tau_2(v)$ is the subsequent processes.

Slow rate process:

In this case let τ_o be the shear strength measured at $v \to 0$ and let us take the relative $\tau_1(v)$ value where – assuming a constant shear surface (A) – the shear stresses can be transformed into shear forces according to Equation (2):

$$\frac{\tau_1(v)}{\tau_o} = \frac{A\tau_1(v)}{A\tau_o} = \frac{F_1(v)}{F_o} \approx \frac{n_1(v)f_1}{n_1(0)f_1} = \frac{n_1(v)}{n_1(0)} = P\left(X \geq h(v)\right) = P\left(h^{-1}(X) \geq v\right) \approx e^{-(v/a_1)^{\beta_1}} \qquad (2)$$

The number of active chains joining the fiber surface and the matrix at a crosshead speed of v is denoted by $n_1(v)$ (at v=0 it corresponds to $n_1(0)$), and that the average resistance force of the tie chains by f_1. By reduction the fraction of active tie chains can be obtained which in turn defines a probability, of which we know that it decreases monotonically with v. Let thus X a statistical strength-like quantity, a kind of shear strength component which is functionally related to the crosshead speed, v (this h function increases monotonically with v and can be inverted). This allows the derivation of a statistical variable $h^{-1}(X)$ the dimension of which is speed-like, being related to the strength. The probability of the fact that this variable is not lower than v decreases monotonically with v. Such probabilities related to strength properties can usually be well described by the Weibull distribution, representing the limiting distribution of minima, the two parameter version of which can be given by Equation (3):

$$\tau_1(v) = \tau_o e^{-(v/a_1)^{\beta_1}} \qquad (3)$$

where a_1 is the so-called scale factor and β_1 is the so-called module factor.

High speed process:

Also here we follow a similar process. τ_∞ is the stabilized shear strength obtained at $v\to\infty$ and τ_2 (v) is related to that – assuming also a constant shear surface (A) – the shear stresses can be transformed into shear forces according to Equation (4):

$$\frac{\tau_2(v)}{\tau_\infty}=\frac{A\tau_2(v)}{A\tau_\infty}=\frac{F_2(v)}{F_\infty}\approx\frac{\left(n_2(0)-n_2(v)\right)f_2}{n_2(0)f_2}=1-\frac{n_2(v)}{n_2(0)}= \\ =P\left(Y<g(v)\right)=P\left(g^{-1}(Y)<v\right)\approx 1-e^{-(v/a_1)^{\beta_1}} \tag{4}$$

$n_2(v)$ denotes the number of active network chains in the matrix layer adjacent to the fiber where the shear deformation is the most intense and the shear failure occurs at a crosshead speed of v, and $n_2(0)$ denotes the number of total network chains in this environment and let us assume that the average resistance force of the network chains is f_2. After reduction in Equation (5) one gets the number of active network chains (more correctly the probability of finding them there), which increases monotonically with v. Similarly to the previous case, let Y is a strength-like statistical variable which is in a monotonically increasing and invertable functional relation with (g) the v deformation rate. Thus one can define a statistical variable, $g^{-1}(Y)$ with the dimension of speed, related to the strength, and the probability of this being lower than v increases monotonically with v. This is also characterized by the Weibull distribution as in Equation (5):

$$\tau_2(v)=\tau_\infty\left(1-e^{-(v/a_1)^{\beta_1}}\right) \tag{5}$$

where a_2 and β_2 are the scale and module factors respectively.

Taking into account Equations (3) and (5) the resultant shear strength is described by Equation (6):

$$\tau(v)=\tau_1(v)+\tau_2(v)=\tau_o e^{-(v/a_1)^{\beta_1}}+\tau_\infty\left(1-e^{-(v/a_1)^{\beta_1}}\right) \tag{6}$$

Fitting the components according to Equation (6) to the measured points the resulting curve is shown in Fig. 5.

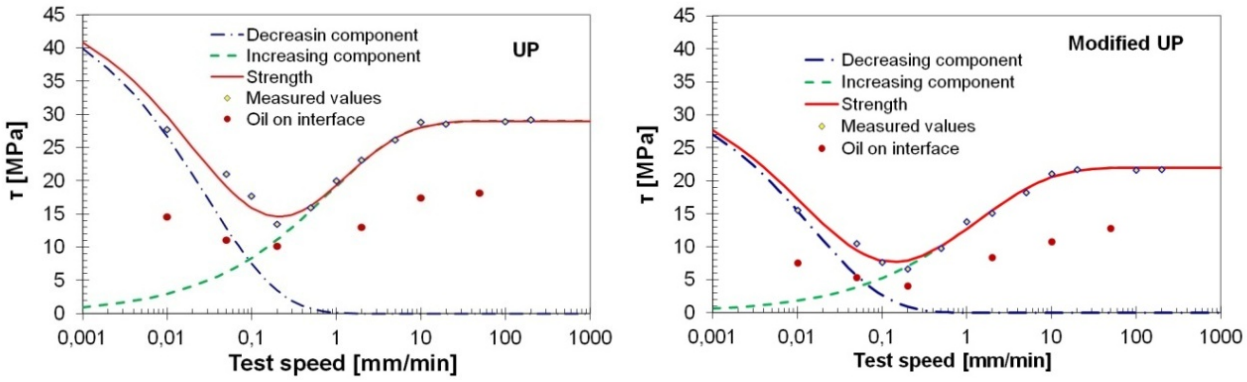

a) b)

Fig. 5. Curves fitted to interfacial strength values measured at different deformation rates for (a) glass fiber-UP and for (b) glass fiber- modified UP

Fitting of the resultant curve to the test results was done by manual iteration, the parameters of the equation are summarized in Table 2, where v* is the test speed belonging to the minimum and R is the correlation ratio. Based on the results it can be observed that the correlation ratios are high (see Tabl 2).

	Starting section			**Later section**			**Complete curve**		
Matrix	τ_o [MPa]	a_1 [mm/s]	β_1 [-]	τ_∞ [MPa]	a_2 [mm/s]	β_2 [-]	$\tau_{min}(v^*)$ [MPa]	v^* [mm/s]	**R** [-]
UP	48	0.029	0.5	29	0.85	0.5	14.6	0.21	0.93
UP_EBRECYL	35	0.015	0.5	22	1.35	0.5	7.7	0.15	0.92

Table 2. Parameters of the equation describing the curve fitted to the measured dependence on the test speed

According to the study the module parameters (β exponents) are identical not only for the given material pair, but also in both cases, their value is uniformly 0.5. This hints at similar mechanism (regarding the deformation of tie chains and network chains), thus corroborating our hypotheses. Plasticization decreased the τ_∞ stationary shear strength of the fiber/UP system, but it did not change the τ_o initial strength, i.e. the number and characteristics of the surface bonds. The scale factor changed, however, it decreased by 50%. It means that the

effect of test speed became more intense, the $\tau_1(v)$ values decreased for the plasticized system for v>0. Plasticization decreased τ_o, the initial shear strength belonging to infinitely low speed by 13 MPa. Plasticization decreased by about 50% the minimum value of the shear strength, and the position of this minimum is at about 25% lower speed.

Effect of geometrical parameters

Fig. 6 shows the effects of the cylinder diameter (D) and of the embedded lengths (L=H) on the shear strength (see Fig. 1.). Two effects can be observed: with decreasing plate thickness the measured interfacial shear strength increases even if the H/D ratio is nearly constant. At the same time, it was observed that the strength value is maximum at a certain H/D ratio for all plate thicknesses investigated.

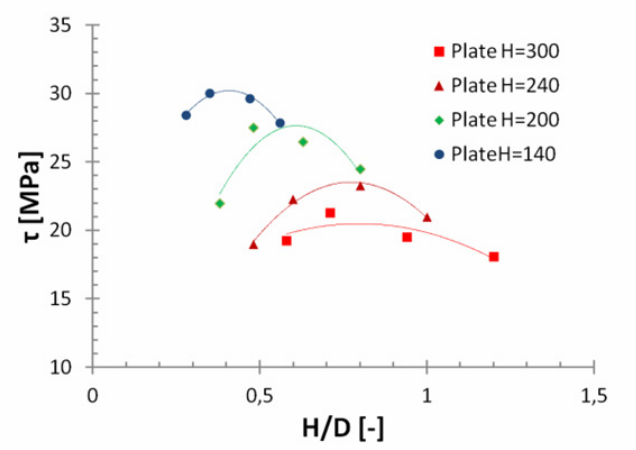

Fig. 6. The effect of the H/D ratio on the measured strength

In the present case, because of technical reasons, there was no chance to vary the above parameters further. Therefore our experimental studies were complemented by finite element modeling (ANSYS v.12.1) to consider those stress effects at such geometrical ratios which could not be realized experimentally (Fig 7a and 7b). A linear material model was used in the calculations. The plate (considered to be stiff) was modeled as a fixed support, between the fiber and matrix perfect bonding was assumed, and loading was introduced by an axial force

located at the end of the fiber. The elements were of quadratic type, their number was between 8-30 thousand, and that of the nodes was between 40-160 thousand, depending on the volume of the specimen. When defining the net we tried to achieve uniform element sizes. Possible deviations caused by finer or coarser elements were checked by separate runs.

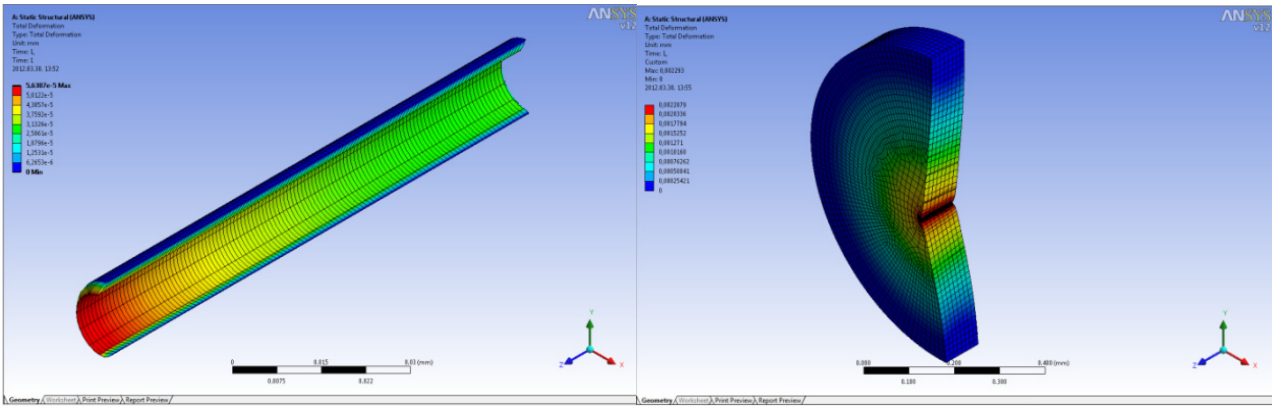

a) 0 b)

Fig. 7. The deformation calculated by the FEM modeling at high (a), and small (b) H/D ratios for the matrix cylinder (the fiber is not plotted for better visibility)

If the embedded length is large, significant deformation and stress differences may arise between the two endpoints of the interface. Of course, as soon as a crack is formed at any position (as in our case above), it will spread along the total interface, so the shear strength will be lower. Therefore test specimens prepared with thinner plates will provide more realistic strength values.

It is important that for each studied H thickness a maximum strength value was observed in the range of H/D=0.4 – 0.8 ratio. If the diameter of the cylinder, D is decreased to the theoretical limit, i.e. to the d_{fiber} diameter, we get pure shear stress, so in principle we could measure pure shear strength. If the D diameter is increased infinitely, a complex stress state is obtained, containing both shear stresses along the fiber direction and radial tensile/compressive stresses perpendicularly to the fiber. The measurable strength belonging

to this stress state must therefore be lower than in the case when d_{fiber} is close to the D borehole diameter. If, however, the infinitely large D diameter is gradually reduced, the radial stress components will also decrease, thus the pure shear stress state is approached and the measured strength will increase. It may be strictly monotonic (i.e. it may not exceed the strength value belonging to the pure shear stress), but instead based on the measurements this relation is exhibits a maximum. Assume that this maximum is caused by the differences in the stress field as a result of changing geometrical ratios, which may be amplified or attenuated by the viscoelastic properties and molecular structure of the polymer material. Finite element modeling, on linear material models also confirmed this theorem.

If the fiber is loaded by a given force at a given specimen geometry, a corresponding stress response is obtained. Let us assume that at this stress level the interface of the test specimen just remains intact. If the same loading is applied to a geometry of different shape and, as a consequence, higher stress arises in response, this second test specimen will bear less load, i.e. the measured interfacial shear strength will also be lower. If at given ratios the calculated stress is lower, the expected strength will be higher. The results of the calculations are shown in Fig. 8.

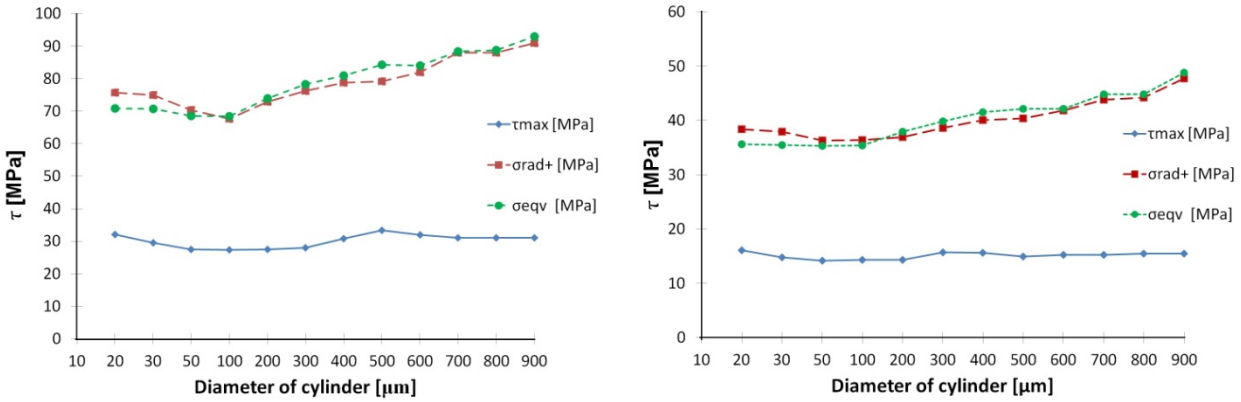

Fig. 8. Stresses obtained by finite element modeling (FEM) for 200 µm embedded fiber length, as a function of the cylinder diameter at (a) 0.05 N and (b) 1 N loading force

When defining the net during modeling, our main concern was to maintain a near constant element size, so that the number of elements belonging to the given diameter remained identical. To check it certain runs were repeated with finer and coarser nets, as well. If the net became finer the calculated maximum values increased, and decreased if the net became coarser, but the shape of the curves did not change. Using properly selected material parameters such stress values were calculated which were somewhat higher than the experimentally obtained. This can be explained by the presence of defects which were not taken into account by the model but actually present in reality (such as foreign materials at the interface, errors of coaxiality, inclination etc.).

It can be observed that at both loading levels around 50 and 100 μm diameters the calculated shear and radial tensile stresses exhibit minima, while this is less observable with the resultant stress. This latter rather increases (although not monotonically). It means that from the shear and radial tensile stresses dominantly initiating the failure around these H/D values, identical (breaking) stresses can be achieved at higher loads, resulting in a higher measurable strength. A new observation is, however, the steady values of the shear stresses at large diameters, as it was not possible to produce test specimens with so low H/D values experimentally. A possible explanation of this phenomenon might be that after reaching a certain diameter the axial load arising at the interface becomes constant. Meanwhile, however the radial and thus the resultant stress increases further, leading to decreasing strength.

Conclusions

We can conclude that in the cylinder test, developed from the microdebond test, the measured interfacial strength is strongly influenced by the test speed (crosshead speed) and by the specimen geometry. The test speed dependence can be explained by the time needed for the molecular structural changes in the polymer material while the size effect by the internal

stress distribution of the test specimens of different shape and size. With increasing crosshead speed the strength first decreases (up to about 0.2 mm/min), then increases linearly with the crosshead speed until we reach a value of about 10 mm/min. Afterwards no more considerable change is observed in the strength values. This phenomenon is the result of two opposing processes. At low deformation rates the chain ends exhibiting secondary bonding to the surface and providing the majority of adhesion forces have time to relax after detachment (breakage of the secondary bond) and new secondary bonds may form (recombination process). Because of the relaxation these processes are limited to the interfaces. With increasing speed the number of recovering secondary bonds decreases but, at the same time, the stressed chains can move further chains within the matrix, extending the effective volume. Because of the energy needed for this process the measurable strength will increase until being limited by the force that can be transmitted at the interface.

With increasing embedded length the measured adhesion force decreases. This is caused by the elasticity of the fiber, as the largest deformation and stress will arise around the entrance point of the fiber, which reaches the load bearing ability of the system even at lower fiber stresses, thus the initiating crack propagates along the interface. At a given embedded length the measured interfacial shear strength values exhibit a maximum at a given cylinder diameter (around H/D=0.4-0.8). Based on finite element simulations for the given geometrical ratios a minimum can be detected for the shear and for the radial tensile stress components assuming constant fiber load, which explains the strength improvement. Of course other phenomena (e.g. molecular structural and viscoelastic properties of the polymers, interfacial properties etc.) may interfere, which should be clarified by further research.

In summary if using cylinder test evaluated by the interfacial shear strength method, if the goal is the experimental determination of the shear strength, it is suggested to use as small H value as possible with a H/D ratio around 0.5. To minimize the error caused by eventual test

speed variations, it is suggested to use test speeds above the saturation speed (in case of the examined materials 10 mm/min).

Acknowledgements

The content of this work is related to the project "Development of coordinated, quality oriented, educational and R+D+I strategy and operational model at the Technical University" supported by the New Széchenyi Plan, under program number TÁMOP-4.2.1/B-09/1/KMR-2010-0002.

References

[1] Zhandarov S, Mäder E (2005) Characterization of fibre/matrix interface strength: applicability of different tests, approaches and parameters. Compos Sci Technol. Doi: 10.1016/j.compscitech.2004.07.003

[2] Bailey C, Davies P, Grohens Y, Dolto G (2004) Application of interlaminar tests to marine composites. A literature review. Appl Compos Mater. Doi: 10.1023/B:ACMA.0000012902.93986.bf

[3] Yu T, Wu CM, Chang CY, Wang CY, Rwei SP (2012) Effects of crystalline morphologies on the mechanical properties of carbon fiber reinforcing polymerized cyclic butylene terephthalate composites. Express Polym Lett. Doi: 10.3144/expresspolymlett.2012.35

[4] Yao M, Deng H, Mai F, Wang K, Zhang Q, Chen F, Fu Q (2011) Modification of poly(lactic acid)/poly(propylene carbonate) blends through melt compounding with maleic anhydride. Express Polym Lett. Doi: 10.3144/expresspolymlett.2011.92

[5] Balogh G, Czigany T (2011) Effect of low UD carbon fibre content on mechanical properties of in situ polymerised cyclic butylene terephtalate. Plast Rubb Compos. Doi: 10.1179/1743289811X12988633927871

[6] Nairn JA (2004) In: Moore D. R. (ed) The application of fracture mechanics to polymers, adhesives, and composites. Elsevier, Amsterdam

[7] Pisanova E, Zhandarov S, Mäder E (2001) How can adhesion be determined from micromechanical tests? Compos Part A-Appl S. Doi: 10.1016/S1359-835X(00)00055-5

[8] Nardin M, Schultz J (1993) Relationship between fibre-matrix adhesion and the interfacial shear strenght in polymer-based composites. Compos Interface. Doi: 10.1163/156855493X00068

[9] Kessler H, Schüller T, Beckert W, Lauke B (1999) A fracture-mechanics model of the microbond test with interface friction. Compos Sci Technol. Doi: 10.1016/S0266-3538(99)00078-0

[10] Liu CH, Nairn JA (1999) Analytical and experimental methods for a fracture mechanics interpretation of the microbond test including the effects of friction and thermal stresses. Int J Adhes Adhes. Doi: 10.1016/S0143-7496(98)00057-8

[11] Schüller T, Bahr U, Beckert W, Lauke B (1998) Fracture mechanics analysis of the microbond test. Compos Part A-Appl S. Doi: 10.1016/S1359-835X(98)00044-X

[12] Morlin B, Czigany T (2012) Cylinder test: Development of a new microbond method. Polymer Testing. Doi: 10.1016/j.polymertesting.2011.10.007

[13] Zinck P, Wagner HD, Salamon L, Gerard JF (2001) Are microcomposites realistic models of the fibre/matrix interface? II. Physico-chemical approach. Polymer. Doi: 10.1016/S0032-3861(00)00871-5

[14] Straub A, Slivka M, Schwartz P (1997) A study of the effects of time and temperature on the fiber/matrix interface strength using the microbond test. Compos Sci Technol. Doi: 10.1016/S0266-3538(96)00146-7

[15] Day RJ, Rodrigez JVC (1998) Investigation of the micromechanics of the microbond test. Compos Sci Technol. Doi: 10.1016/S0266-3538(97)00197-8

[16] Grishchuk S, Karger-Kocsis J (2011) Hybrid thermosets from vinyl ester resin and acrylated epoxidized soybean oil (AESO). Express Polym Lett. Doi: 10.3144/expresspolymlett.2011.2

[17] Pandey G, Kareliya CH, Singh RP (2012) A study of the effect of experimental test parameters on data scatter in microbond testing. J Compos Mater. Doi: 10.1177/0021998311410508

[18] Anuar H, Zuraida A, Morlin B, Kovács JG (2011) Micromechanical property investigations of poly(lactic acid)-kenaf fiber biocomposites. J Nat Fibers. Doi: 10.1080/15440478.2011.550765

[19] Persson BNJ, Volokitin AI (2006) Rubber friction on smooth surfaces. Eur Phys J E. Doi: 10.1140/epje/i2006-10045-9

[20] Vas LM, Rácz Z (2004) Modeling and testing the fracture process of impregnated carbon-fiber roving specimens during bending: Part I – Fiber bundle model. J Compos Mater. Doi: 10.1177/0021998304044767

[21] Mendels DA, Leterrier Y. Manson JAE (2002) The influence of internal stresses on the microbond test- I: Theoretical analysis. J Compos Mater. Doi: 10.1177/0021998302036003508